15th Iranian Hydraulic Conference, 14-15 December 2016
Faculty of Engineering and Technology, Imam Khomeini International University,
Qazvin, Iran

Near field mixing of Multi-Diffuser Dense Jets in Shallow water condition and Ambient Currents

Hassan Akbari[1], Mohammad Hossein Ebrahimi[2]

1- Department of civil engineering, Tarbiat Modarres University, Tehran, Iran
2- Sahel consultant engineering, Tehran, Iran

Akbari.h@modares.ac.ir

Abstract

Desalination plants are effective alternatives for providing required potable waters. Since outfall of these plants can be harmful for marine environments, it is desirable to use an optimum diffuser geometry with maximum dilution effect. A multiple diffuser system with a proper geometry is usually a good solution. In this study, the pollutant behavior of such a system in shallow water condition is investigated by making use of Computational Fluid Dynamic (CFD) method. An actual case is taken into account and both matching and opposite ambient currents are also simulated. It is concluded that the tail of the jet as well as its height and traveling length can be affected by ambient current, yet multi-diffuser jets are less sensitive to current than a single port system. It is also shown that simulating the pressure loss is an important item in designing an outfall system.

Keywords: Desalination, near field, multi diffuser, shallow water, ambient current.

15Hydro-1153

1. INTRODUCTION

Construction of desalination plants has been increased recently to response to the expanding potable water demand for economic and community activities as well as utility consumptions. Since a desalination plant is a reliable and a cost-effective alternative for providing required source of water [1], there has been a rapid growth in both size and number of these plants in the recent years [2]. However, desalinations plants have some potential effects on marine environment due to the disposal of brine discharges into the sea that generate a risk for the quality of coastal waters and the marine life [3].

The behavior of an effluent discharge is complicated and it depends on several physical phenomena such as dispersion, diffusion, convection and buoyancy of disposal water. The importance of these parameters changes according to the distance from the effluent discharge. Generally two near field and far field regions can be detected with different spatial and time scales [4]. In the vicinity of the outflow system, a mixing jet with noticeable turbulences dominates the flow. This region is defined as the near field region and at the far field region starts at the end of the near field region where the turbulence effect collapses. [5]. In the far field region, brine water forms a gravity driven current at the sea bed and the main mixing processes are advection and diffusion [6]. Nearfield modeling is too important because the most part of the dilution occurs in this region. Several numerical and experimental studies have been done for investigating the generated brine jet trajectory from a single riser and its dilution process in vicinity of the effluent discharge. The numerical studies can be classified in three basic approaches as discussed in [7], i.e.: (a) Models based on the dimensional analysis of the relevant processes, (b) Models based on the integration of differential equations, and (c) Computational Fluid Dynamics (CFDs) models. The simplest method among these methods is the dimensional analysis of experimental data and considering independent variables with greater influences on the jet pattern. CORMIX1 [8], and CORMIX2 [9] as two modules of the commercial CORMIX software [10] work based on this approach. In the second method, a simple differential equation is derived by integrating the governing equations over a cross section and distribution of the parameters around the jet axis is obtained based on assuming a Top hat or Gaussian distribution function. Several commercial software have been developed based on this approach such as JetLag of VISJET software [11] CORJET of CORMIX software [12,13]; and UM3 of VISUAL PLUMES [14].

The ability of the above mentioned models in modeling negatively buoyant jets are compared in [15] and it was concluded that these models are not able to model dense jets accurately. It was shown that CORMIX1, CORJET and MEDVSA are very conservative models that results always in a lower salinity than the measurements. However, UM3 was the only model that results in a higher salinity than the measured salinity along the jet axis [16]. In comparison with these simplified approaches, CFD tools provide rigorous platforms with fewer simplification assumptions, yet, with higher computational costs. Navier-Stokes and transport equations are solved in CFD models and it is possible to apply different turbulence closure models such as k-epsilon, large eddy simulation or other complex models for modeling jet disturbance with considerable Reynold number. Meanwhile, few studies have been done to model brine jets by making use of CFD models and most of these studies have considered the behavior of a single effluent jet [17, 18].

Actually, researchers usually have utilized simplified models and most of the studies have been done to find an acceptable inclined port angle for a single port condition. For example, a 60° angle was suggested to provide the longest trajectory and the highest dilution in comparison with the port angles of 30°, 45°, and 90° [19]. Later, it was concluded based on experiments that the dilution is not sensitive to the port angles in the range of 45° to 65° [20]. However, the dilution corresponding to a 60°-angle was yet slightly higher at the end of the near field region. These studies were, however done for deep waters where the trajectory does not interact with the water surface. By modeling a single jet behavior in a shallow water condition, it was concluded that a 30°-port is preferred than other angles [21]. Since few studies have been done for investigating the jet behavior for either multi-port systems or shallow water conditions particularly by utilizing CFD models, in this research, the behavior of a multi-port system in shallow waters is studied by means of the Fluent software as one of the well-known CFD models. For this purpose, flow rates and water depths of an actual condition corresponding to the desalination system of Kangan petrochemical plant in Iran is taken into account.

2. GOVERNING EQUATIONS

The continuity and momentum equations are solved besides the transport equation as the governing equations. The fluid density changes during simulations as a function of salinity and the k- ε model is applied in Fluent software [22] to simulate the turbulence effects. Since the effect of global phenomena such as wind and waves are not significant in the flow behavior in a near field region, these parameters are not modeled in this study. The governing equations for a 3-D simulation are [22]:
Continuity equation:

$$\frac{\partial r}{\partial t}+\frac{\partial}{\partial x}(ru)+\frac{\partial}{\partial y}(rv)+\frac{\partial}{\partial z}(rw)=0 \qquad (1)$$

Momentum equation in a -direction:

$$\frac{\partial ru^a}{\partial t}+\frac{\partial}{\partial x}(ruu^a)+\frac{\partial}{\partial y}(rvu^a)+\frac{\partial}{\partial z}(rwu^a)=rg_a-\frac{\partial P}{\partial a}+\frac{\partial}{\partial x}\left(m_e\frac{\partial u^a}{\partial x}\right)+\frac{\partial}{\partial y}\left(m_e\frac{\partial u^a}{\partial y}\right)+\frac{\partial}{\partial z}\left(m_e\frac{\partial u^a}{\partial z}\right)+R_a+T_a \qquad (2)$$

Where u, v, and w are velocity components in x, y and z directions, respectively and u^a is the velocity component in a direction, (for example in y-direction $u^a=v$). ; ρ, μ and μe are the seawater density, dynamic viscosity and effective viscosity of flow, respectively. R_a is source term in a direction, which is not implemented in this study. g_a is the components of the gravity vector. T_a is the viscous loss term which is formulated as:

$$T_a=\frac{\partial}{\partial x}\left(m\frac{\partial u}{\partial a}\right)+\frac{\partial}{\partial y}\left(m\frac{\partial v}{\partial a}\right)+\frac{\partial}{\partial z}\left(m\frac{\partial w}{\partial a}\right) \qquad (3)$$

To calculate the effective viscosity, k- ε turbulence model is used as:

$$\frac{\partial}{\partial t}(rk)+\frac{\partial}{\partial x}(ruk)+\frac{\partial}{\partial y}(rvk)+\frac{\partial}{\partial z}(rwk)=\frac{\partial}{\partial x}\left(\frac{m_t}{s_k}\frac{\partial k}{\partial x}\right)+\frac{\partial}{\partial y}\left(\frac{m_t}{s_k}\frac{\partial k}{\partial y}\right)+\frac{\partial}{\partial z}\left(\frac{m_t}{s_k}\frac{\partial k}{\partial z}\right)$$
$$+m_t f-re+\frac{C_4 b m_t}{s_t}\left(g_x\frac{\partial T}{\partial x}+g_y\frac{\partial T}{\partial y}+g_z\frac{\partial T}{\partial z}\right) \quad (4)$$

$$\frac{\partial}{\partial t}(re)+\frac{\partial}{\partial x}(rue)+\frac{\partial}{\partial y}(rve)+\frac{\partial}{\partial z}(rwe)=\frac{\partial}{\partial x}\left(\frac{m_t}{s_e}\frac{\partial e}{\partial x}\right)+\frac{\partial}{\partial y}\left(\frac{m_t}{s_e}\frac{\partial e}{\partial y}\right)+\frac{\partial}{\partial z}\left(\frac{m_t}{s_e}\frac{\partial e}{\partial z}\right)$$
$$+C_{1e}m_t\frac{e}{k}j-C_2 r\frac{e^2}{k}+\frac{C_m(1-C_3)brk}{s_t}\left(g_x\frac{\partial T}{\partial x}+g_y\frac{\partial T}{\partial y}+g_z\frac{\partial T}{\partial z}\right) \quad (5)$$

Where; $m_t(=rC_m k^2/e)$ is the turbulent viscosity; κ and ε are turbulent kinetic energy and its dissipation rate, respectively and T is temperature. The proposed value of constants in this turbulent model (C1ε, C2, C3, C4, Cμ), turbulent Prandtl numbers (σk, σε, σt) and thermal expansion β are presented in Table 1.

Table 1- Constants in k- ε turbulence model

$C_m=0.09$	$C_{1e}=1.44$	$C_2=1.92$	$C_3=1.0$	$C_4=0.0$
$s_k=1.0$	$s_e=1.3$	$s_t=0.85$	$b=0.0$	

Transport equation

$$\frac{\partial rS}{\partial t}+\frac{\partial}{\partial x}(ruS)+\frac{\partial}{\partial y}(rvS)+\frac{\partial}{\partial z}(rwS)=\nabla.\left[\left(rD_m+\frac{m_t}{SC_t}\right)\nabla S+D_s\nabla T\frac{\nabla T}{T}\right]+S_s \quad (6)$$

Where; $SC_t=(m_t/rD_t)$ is the turbulent Schmidt number with a default value of 0.7. This parameter controls the turbulent diffusivity that is much higher than the laminar diffusion in a jet flow. S is mass fraction represents salinity and Ss is the source term. Dm and Ds are the mass diffusion and the thermal diffusion coefficients, respectively.

3. GEOMETRY AND BOUNDARY CONDITIONS

Since up to 90% of dilution occurs in nearfield region due to the initial momentum of the effluent discharge [23], configuration of the outfall system make an important role in achieving an optimum total dilution. In this study, an actual case is selected for investigating the jet behavior of a multi diffuser system in shallow waters by taking into account the ambient current condition. Up to now, few studies have been done for this purpose particularly by means of CFD models. Since brine contains more salt than fresh seawater, its density is higher than seawater density and therefore, the effluent jet tends to return to the seabed. Dilution, however, occurs during this process. Schematic diagram of an outfall system is shown in Figure 1. As shown in this figure, discharge point is located 500 m far from the shoreline at the depth of 5 m corresponding to mean sea level (MSL). The elevation of the nozzles is 2.9 m above the sea bed that means that 2.1 m of water column exists above the nozzles. The desalination system is located in Kangan area at the southern coast of Iran. Brine discharge and density of this desalination plant are 15000 m³/h and 1045 kg/m³, respectively while the fresh seawater density is 1024 kg/ m³. In this area, tidal currents are dominant and since a shallow water condition is selected for study, the currents are generally parallel to the shoreline. At the outfall point, the maximum and the averaged current velocity at the seabed are 0.5 m/s and 0.1 m/s, respectively and ambient current exceeds 0.05m/s more than 90% of the time. Since it is advised to consider a minimum permanent current velocity [23] in investigating the most critical dilution effect, the ambient current velocity is selected as 0.05m/s. It should be noted that dilution increases in presence of higher ambient currents. Parts of an outfall system have been shown in Figure. 1.

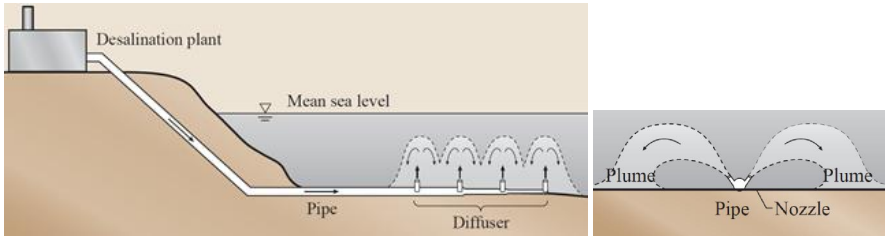

Figure 1. diagram of an Outfall System

Arrangement of the simulated outfall risers is shown in Figure 2. As shown in this figure, 15 outlet nozzle are installed on 60 m of the pipe. Outlet velocity at discharge nozzles shall be high enough to maximize the dilution at near-filed. On the other hand, the velocity should be in a practical range. In this study, outlet velocity at each nozzle is assigned 4 m/s by selecting the inner diameter of each nozzle as 310 mm. Nozzles aligned at 45-degree compare to shoreline and 15 degree compare to horizon. This angle is selected in such a way that the rise height to the jet's upper boundary be less than approximately 90% of the water depth to avoid deleterious effect of surface contact on dilution [24]. In deeper location, however, higher angles can be used and an incline angle of 60-degree compare to horizon results in the highest dilution in deep waters [24]. For modeling the pipe and risers, tetrahedral elements are used for meshing the most areas of the surrounding sea and triangular meshing is used for nozzles and other more complicated sea regions. The used mesh includes of 1597375 cells in total with edge dimension ranges from 50 to 400 mm. The ambient current with -0.05 m/s velocity in y direction (parallel to the shoreline) is utilized at the inlet of the domain. The water density (representative of salinity) at the inlet boundary is set equal to the seawater density (ρ =1024 kg/m3 and S0 = 40,000 ppm) with no gradient while the flow velocity and brine density at the discharge point are constant during the simulation. The pressure outlet condition is utilized at the outlet boundary and the two other lateral boundaries (nearshore and offshore boundaries) are modeled by the symmetrical condition. The non-slip wall condition is used for modeling sea bottom and the normal gradient of velocity is set to zero at the free surface boundary. The residuals of the continuity and momentum equations are selected as 10−4 to ensure satisfy the convergence criteria.

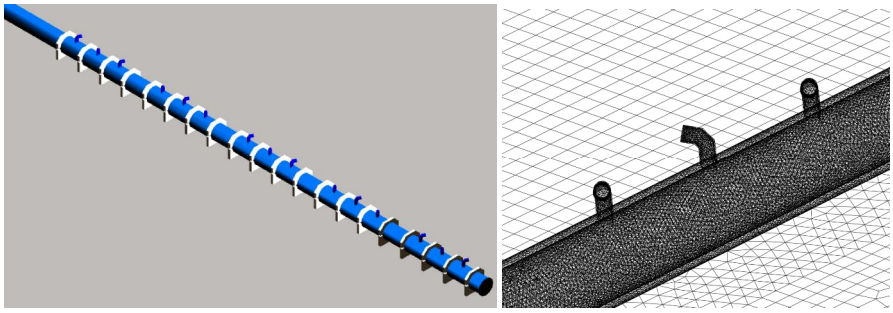

Figure 2. Geometry of nozzle pipes and the utilized mesh

As shown in Figure 1, a weir box is also used to provide the required head and to eliminate the air entrapment in the pipes by minimizing the air entrainments. This weir box, actually ensure that the inlet and outlet pipes are always submerged. Since the total head loss of an outfall system is the summation of the head losses in pipe, riser system and weir box, the flow inside the weir box is also simulated by means of Fluent software. For this purpose, tetrahedral meshing is used for most areas of the weir box and triangular meshing is used for the weir edges as well as for other complicated regions. The model geometry and elements are shown in Figure 3. The weir box is a double compartment pound with two different bed levels. The brine water comes to the weir box via two inlet pipes with 064 and 0.76 m internal diameter and goes to the outfall risers via one pipe with 1.60 m internal diameter. The utilized mesh includes 561554 cells with edge dimension ranges from 50 to 150 mm.

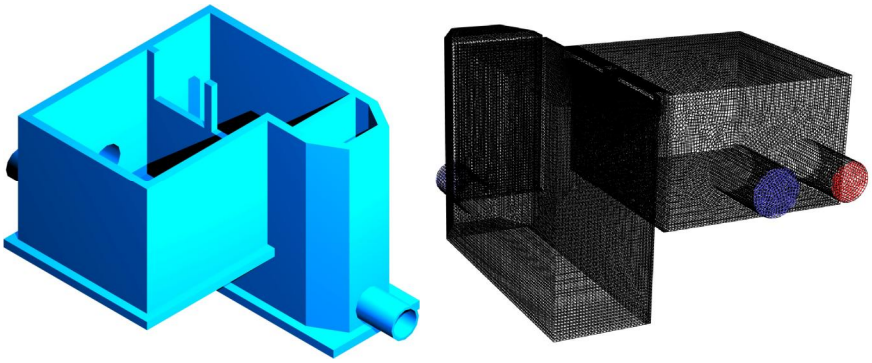

Figure 3. Geometry of weir box and the utilized mesh

4. SIMULATED FLOW AROUND RISERS

The hydraulic of the nozzle pipes and the behavior of the jet plume are modeled using Fluent software. Counters of velocity magnitude in a horizontal section at the level of nozzles and in a vertical section perpendicular to the main pipe section are presented in Figure 4. Contours of density in similar sections are shown in Figure 5. The pattern of both velocity and density distributions presented in these figures are nearly the same and follow the jet plume. Although the magnitude of the ambient velocity (-0.05 m/s in y-direction) is negligible than the jet discharge velocity (4.0 m/s), it affects the pollution pattern slightly even at the level of nozzles. As it can be seen in Figure 4, the velocity contours are longer in the –y direction that is parallel to the ambient current direction. It means that the horizontal length of the jet plume (from discharge point to the returning point of the jet) is longer for a jet outflow matching with the direction of the ambient current and shorter for an opposite current direction. Rise height of the jet plume decreases, however, in the case of matching ambient currents. The end parts of the velocity contours of the jets at the upper part in Figure 4 (those interact with an opposite current) are inclined downward due to interaction with ambient current. The jet velocity is decreased at its tail and the jet route is therefore more sensitive to the ambient current parameters. In addition, the maximum effect of the ambient current on the jet plume occurs for the generated jet form the first diffuser. Actually, the uniformity of the ambient current is preserved at the initial parts of the main pipe while the ambient current is completely disturbed at the middle parts of the main pipe due to the interaction of the multiple jets with the ambient current. As a result, the ambient current is stronger and less disturbed at the initial parts and its influence on the jet pattern is clearly more sensible. On the other hand, the jet plumes are less affected by the ambient current at the middle parts of the main pipe where the jet velocity is completely dominant over the ambient current. This outcome means that a single jet is more vulnerable to the ambient current than a multi-diffuser jet.

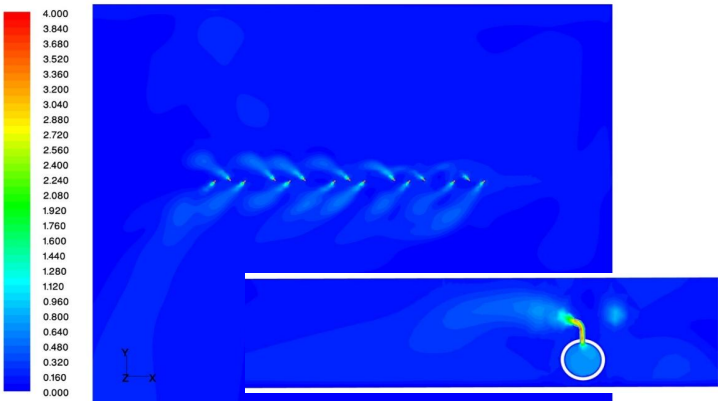

Figure 4. Counters of velocity magnitude; a) at nozzles i.e. 2.9 m form seabed; b) at a vertical section

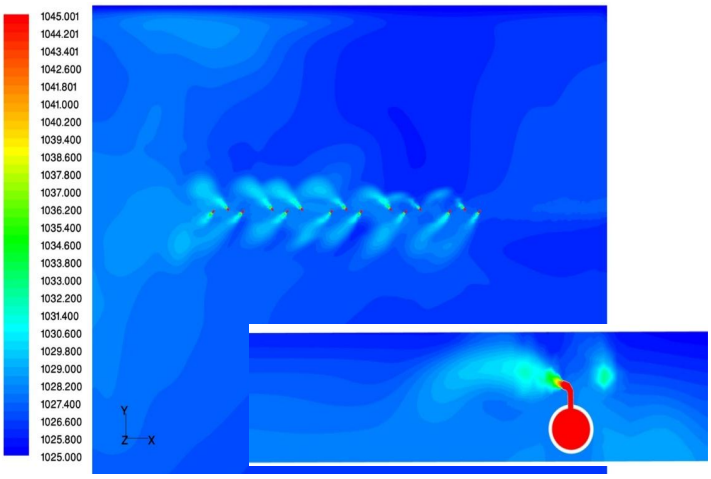

Figure 5. Counters of density; a) at nozzles i.e. 2.9 m form seabed; b) at a vertical section

Velocity contours along the main pipe and diffusers are presented in Figure 6. As shown in this figure, the outfall velocity decreases along the main pipeline due to decreased discharges at the end parts, however, velocity at all the nozzles are nearly constant with the magnitude of 4.0 m/s. Total head loss of nozzle pipe and nozzles is 1.85 m.

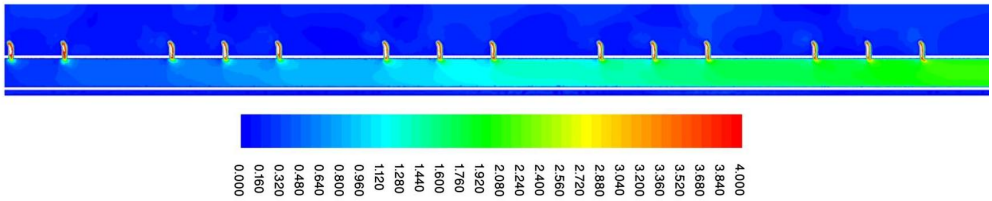

Figure 6. Counters of velocity magnitude at the vertical section through nozzle pipe

5. SIMULATED FLOW THROUGH WEIR BOX

To calculate the total head loss of an outfall system it is required to calculated the head loss in the weir box in addition to the head loss due to the diffusers. To do this, the flow inside the weir box is modeled and the results showing the velocity inside the weir box are shown in Figure 7. Maximum velocities occur inside the inlet and outlet pipes as well as over the weirs. Absolute pressures in vertical sections of the weir box through inlet and outlet pipes are presented in Figure 8. By subtracting the outlet pressure from inlet pressure, it can be concluded that the total head loss inside the weir box is 0.51 m. This head loss is nearly one-fourth of the head loss of diffusers.

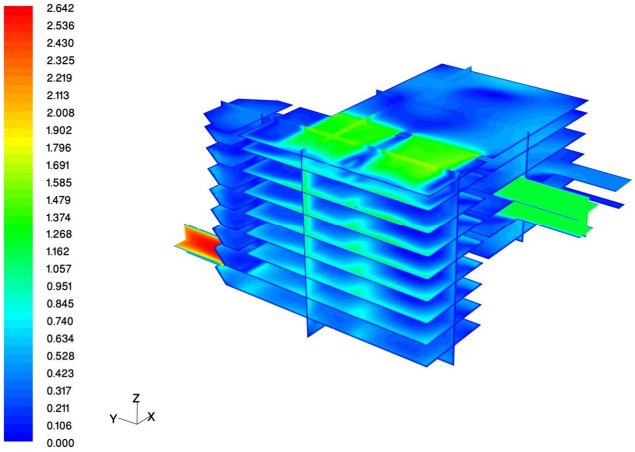

Figure 7. Contours of velocity magnitude in some selected horizontal and vertical sections of the weir box

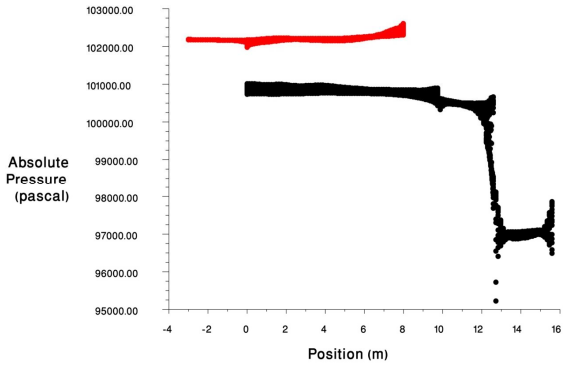

Figure 8. absolute pressure in vertical sections of the weir box through inlet and outlet pipes

6. CONCLUSION

Jet flow from a multi diffuser system is studied numerically by means of Fluent software. An actual case is taken into account and the effect of the ambient current velocity is investigated by modeling a frequent current coincide and opposite to the jet outflow direction. In addition, the flow across the weir box is modeled to investigate the relative contributions of each part of an outflow system in the total head loss of the system, which depends on the losses in weir box, transferring pipe and diffuser pipes. All of these losses should be considered in calculating the required total head behind the hydraulic system in a way to achieve a desired condition with a determined flow rate into the sea. Among these terms, the pressure loss due to the transferring pipes is a function of pipe length which can be different in one case to another one. However, it is resulted that the head losses due to the diffusers take an important part of the total head loss. It is concluded based on the numerical results that:

- Dilution of salinity follow the pattern of the jet velocity distribution in the sea and the pattern of the density contours are nearly the same as the pattern of the velocity contours.
- If the ambient current direction math with the jet flow direction, the horizontal length of the jet plume will be increased and its maximum height will be decreased in comparison with a condition with no ambient current. On the other hand, if an outflow jet encounters an opposite ambient current, its horizontal traveling length and its maximum height will be decreased and increased, respectively.
- Ambient current, even with a small velocity, affects the jet pollution pattern even at the level of the nozzles. This influence, however, depends on the magnitude of the ambient current relative to the jet outfall velocity. Near the outfall nozzles in the near field region, the jet velocity is more dominant than the ambient current, while far from the nozzles the jet velocity is decreased and the jet plume affect clearly from the ambient current. The tail of the jet plume, therefore, can be inclined in accordance with the ambient current.

- A single jet is more affected by ambient current than multi diffuser jets because the pattern of the ambient current will be disturbed near multiple jets.
- In a multi diffuser condition, the jet plume of the first diffuser on the main pipeline has the highest degree of sensitivity to the ambient current.
- The head loss due to diffusers is nearly four times the total head loss of the flow inside the weir box.

6. REFERENCES

1. Bleninger, T., Jirka, G.H., (2009). Environmental Planning, Prediction and Management of Brine Discharges from Desalination Plants.

2. Lattemann, S., Kennedy, M.D., Schippers, J.C., Amy, G., (2010). Chapter 2 Global desalination situation, Sustainability Sci. Eng. 2, http://dx.doi.org/10.1016/S1871-2711(0900202-5)

3. Kikkert, G.A., Davidson, M.J., Nokes, R.I. (2007). Inclined Negatively Buoyant Discharges, J. Hydraul. Eng. 133, 545–554;

4. Kim, A.Y.D., Kang, S.W., Oh, B.C. (2002). Jet Integral–Particle Tracking Hybrid Model for Single Buoyant Jets, J. Hydraul. Eng. 128, 753.

5. Bleninger, T., Jirka, G. (2004). Near-and far-field model coupling methodology for wastewater discharges, Environmental hydraulics and sustainable water management, 2004, 447–453.

6. Randall R.E. (1981). Measurement of a negatively buoyant plume in the coastal waters off Freeport, Texas, Ocean Eng. 8 (4), 407–419.

7. Palomar, P., Lara, J.L., Losada, I.J. (2012). Near field brine discharge modeling part 2: Validation of commercial tools, Desalination 290, 28–42.

8. Doneker, R.L., Jirka, G.H. (1990). Expert System for Hydrodynamic Mixing Zone Analysis of Conventional and Toxic Submerged Single Port Discharges (CORMIX1), Technical Report EPA 600-3-90-012, U.S. Environmental Protection Agency (EPA)

9. Akar, P.J., Jirka, G.H. (1991). CORMIX2: An Expert System for Hydrodynamic Mixing Zone Analysis of Conventional and Toxic Submerged Multiport Diffuser Discharges, U.S. Environmental Protection Agency (EPA), Office of Research and Development.

10. Doneker, R.L., Jirka, G.H. (2001). CORMIX-GI systems for mixing zone analysis of brine wastewater disposal, Desalination, 139, 263–274.

11. Lee, J.H.W., Cheung, V. (1990). Generalized Lagrangian model for buoyant jets in current, J. Environ. Eng. ASCE 116 (6), 1085–1106.

12. Jirka, G.H. (2004). Integral model for turbulent buoyant jets in unbounded stratified flows. Part I: The single round jet, Environ. Fluid Mech. ASCE 4 (2004) 1–56.

13. Jirka, G.H. (2006). Integral model for turbulent buoyant jets in unbounded stratified flows. Part II: Plane jet dynamics resulting from multiport diffuser jets, Environ. Fluid Mech. 6, 43–100.

14. Frick, W.E. (2004). Visual Plumes mixing zone modelling software, Environmental & Modelling Software, 19, 645–654. http://www.epa.gov/ceampubl/swater/vplume/.

15. Palomar, P., Lara, J.L., Losada, I.J., Rodrigo, M., Alva´rez, A. (2012). Near field brine discharge modeling part 1: Analysis of commercial tools, Desalination 290, 14–27.

16. Loya-Ferna´ndez, A., Ferrero-Vicente, L.M., Marco- Mendez, C., Martinez-Garcia, E., Zubcoff, J., Sanchez- Lizaso, J. L. (2012). Comparing four mixing zone models with brine discharge measurements from a reverse osmosis desalination plant in Spain, Desalination 286, 217–224.

17. Al-Sanea, S., Orfi, J., Najib, A. (2015). Numerical study of flow, temperature, and salinity distributions of a brine discharge problem, Desalination and Water Treatment, 55:12, 3218-3230, DOI: 10.1080/19443994.2014.940658.

18. Oliver, C.J., Davidson, M.J., Nokes, R.I. (2013). Predicting the near field of desalination discharges in a stationary environment, Desalination 309, 148–155.

19. Zeitoun, M. A., Reid, R. O., McHilhenny, W. F., and Mitchell, T. M. (1972). Model studies of outfall systems for desalination plants. Part III. Numerical simulation and design consideration. Research and Development Progress Rep. No. 804, Office of SalineWater, U.S. Dept. of the Interior, Washington, DC.

20. Abessi, O., Roberts, P.J.W. (2015). Effect of nozzle orientation on dense jets in stagnant environments. J. Hydraul. Eng., 10.1061/ (ASCE) HY.1943-7900.0001032, 06015009.

21. Abessi, O., Roberts, P.J.W. (2015). Dense Jet Discharges in Shallow Water. Journal of Hydraulic Engineering, ASCE, 142 (1), ISSN 0733-9429/04015033(13), DOI: 10.1061/(ASCE)HY.1943-7900.0001057

22. Fluent 13. Available from: www.ansys.com.

23. Tate, P.M., Scaturro, S., Cathers, B, (2016). Springer handbook of ocean engineering, Part C, Coastal design, Section 32, Marine Outfalls. ISBN: 978-319-16648-3, 2016.